arXiv:1601.00454v3 [hep-ph] 25 Jun 2016

Higgs boson production in the $U(1)_{B-L}$ model at the ILC

Jinzhong Han[1],* Bingfang Yang[2,3],† Ning Liu[2],‡ and Jitao Li[1]

[1] *School of Physics and Telecommunications Engineering, Zhoukou Normal University, Henan, 466001, China*

[2] *College of Physics and Electronic Engineering, Henan Normal University, Xinxiang 453007, China*

[3] *School of Materials Science and Engineering, Henan Polytechnic University, Jiaozuo, 454000, China*

Abstract

In the framework of the minimal $U(1)_{B-L}$ extension of the Standard Model, we investigate the Higgs boson production processes $e^+e^- \to ZH$, $e^+e^- \to \nu_e\bar{\nu_e}H$, $e^+e^- \to t\bar{t}H$, $e^+e^- \to ZHH$ and $e^+e^- \to \nu_e\bar{\nu_e}HH$ at the International Linear Collider (ILC). We present the production cross sections, the relative corrections and compare our results with the expected experimental accuracies for Higgs decay channel $H \to b\bar{b}$. In the allowed parameter space, we find that the effects of the three single Higgs boson production processes might approach the observable threshold of the ILC. But the Higgs signal strengths $\mu_{b\bar{b}}$ of the two double Higgs boson production processes are all out of the observable threshold so that these effects will be difficult to be observed at the ILC.

PACS numbers: 14.80.Ec, 12.60.-i, 13.66.Fg, 12.60.Fr

*Electronic address: hanjinzhong@zknu.edu.cn

†Electronic address: yangbingfang@htu.edu.cn

‡Electronic address: wlln@mail.ustc.edu.cn

I. INTRODUCTION

In the summer of 2012, a bosonic resonance with a mass around 125 GeV was found at the Large Hadron Collider (LHC) by the ATLAS and CMS Collaborations [1, 2]. So far, its properties are compatible with the predictions of the Standard Model (SM) Higgs boson. Meanwhile, the current LHC data is limited, there are still large uncertainties about the couplings between the Higgs boson and the other SM particles [3–7]. Due to the complicated background, the precision measurements of the properties of the Higgs boson at the LHC are severely challenged. By contrast, the Higgs factories beside the LHC, such as the International Linear Collider (ILC) [8–10], can measure the Higgs boson with high accuracy. In many cases, the ILC can significantly improve the LHC measurements due to its clean environment.

The ILC technical design report has pointed that it is planed to measure Higgs boson at three center-of-mass (c.m.) energy: 250 GeV, 500 GeV and 1000 GeV. In the first stage for $\sqrt{s} = 250$ GeV, the precision Higgs program will start at the Higgs-strahlung process $e^+e^- \to ZH$, the cross section for this process is dominant at the low energy and has the maximum cross section at around $\sqrt{s} = 250$ GeV. In the second stage for $\sqrt{s} = 500$ GeV, the two very important processes $e^+e^- \to t\bar{t}H$ and $e^+e^- \to ZHH$ are become accessible. For the process $e^+e^- \to t\bar{t}H$, in which the top Yukawa coupling appears at the tree-level for the first time at the ILC, it will play an important role for the precision measurements of the top quark Yukawa coupling. For the process $e^+e^- \to ZHH$, to which the triple Higgs boson coupling contributes at the tree-level, it will be crucial to understand the Higgs self-coupling and the electroweak symmetry breaking. In the third stage for $\sqrt{s} = 1000$ GeV, the processes $e^+e^- \to t\bar{t}H$, $e^+e^- \to \nu_e\bar{\nu}_eH$ and $e^+e^- \to \nu_e\bar{\nu}_eHH$ are involved. In such energy stages, the channels $t\bar{t}H$ and $\nu_e\bar{\nu}_eH$ have large cross section, and the channel $\nu_e\bar{\nu}_eHH$ can be used together with the ZHH process to improve the measurement of the Higgs self-coupling. So far, many relevant works mentioned above have been extensively studied in the context of the SM [11–17] and some new physics models [18–37].

The minimal $B-L$ extension of the SM is based on the structure $SU(3)_C \times SU(2)_L \times U(1)_Y \times U(1)_{B-L}$ gauge symmetry, in which the SM gauge has a further $U(1)_{B-L}$ group related to the Baryon minus Lepton $(B-L)$ gauged number [38, 39]. It was known

that this model is in agreement with the current experimental results of the light neutrino masses and their large mixing. The $B-L$ model predicted some new particles beyond the SM, such as the new heavy gauge bosons, the heavy neutrino and the heavy neutral Higgs boson. In addition, some couplings of the Higgs boson in the $B-L$ model are modified with respect to the SM. These new effects will alter the property of the SM Higgs boson and influence various SM Higgs boson processes, making the model phenomenologically rich and testable at the LHC and the ILC [39–49]. In this paper, we mainly study the single Higgs boson production processes $e^+e^- \to ZH$, $e^+e^- \to \nu_e\bar{\nu_e}H$, $e^+e^- \to e^+e^-H$, $e^+e^- \to t\bar{t}H$ and the double Higgs boson production processes $e^+e^- \to ZHH$, $e^+e^- \to \nu_e\bar{\nu_e}HH$ in the $B-L$ model at the ILC.

The paper is organized as follows. In Sec.II we briefly review the basic content of the $B-L$ model related to our work. In Sec.III and Sec.IV we respectively investigate the Higgs boson production processes and the Higgs signal strengths in the $B-L$ model at the ILC. Finally, we give a summary in Sec.V.

II. A BRIEF REVIEW OF THE B-L MODEL

Here we will briefly review the ingredients relevant to our calculations, the detailed description of the $B-L$ model can be found in Refs. [40, 43]. The $B-L$ model is the minimal extensions of the SM [50–54] with the classical conformal symmetry, and based on the gauge group $SU(3)_C \times SU(2)_L \times U(1)_Y \times U(1)_{B-L}$. The Lagrangian for the fermionic and kinetic sectors are given by

$$\begin{aligned}\mathcal{L}_{B-L} &= i\ \bar{l}D_\mu\gamma^\mu l + i\ \bar{e}_R D_\mu\gamma^\mu e_R + i\ \bar{\nu}_R D_\mu\gamma^\mu\nu_R \\ &\quad -\frac{1}{4}W_{\mu\nu}W^{\mu\nu} - \frac{1}{4}B_{\mu\nu}B^{\mu\nu} - \frac{1}{4}C_{\mu\nu}C^{\mu\nu}. \end{aligned} \tag{1}$$

The covariant derivative D_μ is different from the SM one by the term $ig'Y_{B-L}C_\mu$, where g' is the $U(1)_{B-L}$ gauge coupling constant, Y_{B-L} is the $B-L$ charge, and $C_{\mu\nu} = \partial_\mu C_\nu - \partial_\nu C_\mu$ is the field strength of the $U(1)_{B-L}$.

The Lagrangian for the Higgs and Yukawa sectors are given by

$$\begin{aligned}\mathcal{L}_{B-L} &= (D^\mu\phi)(D_\mu\phi) + (D^\mu\chi)(D_\mu\chi) - V(\phi,\chi) \\ &\quad -\Big(\lambda_e\bar{l}\phi e_R + \lambda_\nu\bar{l}\tilde{\phi}\nu_R + \frac{1}{2}\lambda_{\nu_R}\bar{\nu^c}_R\chi\nu_R + h.c.\Big). \end{aligned} \tag{2}$$

The $U(1)_{B-L}$ and $SU(2)_L \times U(1)_Y$ gauge symmetries can be spontaneously broken by a SM singlet complex scalar field χ and a complex $SU(2)$ doublet of scalar fields ϕ, respectively.

The scalar potential $V(\phi, \chi)$ is given by

$$V(\phi,\chi) \;=\; m_1^2\phi^\dagger\phi + m_2^2\chi^\dagger\chi + \lambda_1(\phi^\dagger\phi)^2 + \lambda_2(\chi^\dagger\chi)^2 + \lambda_3(\chi^\dagger\chi)(\phi^\dagger\phi). \tag{3}$$

To determine the condition for the potential to be bounded from below, the couplings λ_1, λ_2 and λ_3 should be related with $4\lambda_1\lambda_2 - \lambda_3 > 0, \lambda_1 \geq 0, \lambda_2 \geq 0$. The vev's, $|\langle\phi\rangle| = v/\sqrt{2}$ and $|\langle\chi\rangle| = v'/\sqrt{2}$, are then given by

$$v^2 = \frac{4\lambda_2 m_1^2 - 2\lambda_3 m_2^2}{\lambda_3^2 - 4\lambda_1\lambda_2}, \qquad v'^2 = \frac{-2(m_1^2 + \lambda_1 v^2)}{\lambda_3}. \tag{4}$$

where v and v' are the electroweak symmetry breaking scale and the $B-L$ symmetry breaking scale, respectively.

After the electroweak symmetry breaking, one obtains the mass of the gauge bosons

$$\begin{aligned} m_\gamma &= 0, \\ m_{W^\pm} &= \frac{1}{2}vg, \\ m_Z &= \frac{v}{2}\sqrt{g^2 + g_1^2}, \\ m_{Z'} &= 2v'g'. \end{aligned} \tag{5}$$

where g and g_1 are the $SU(2)_L$ and $U(1)_Y$ gauge couplings. The Z' boson mass is constrained from the most recent limit at LEP [55]

$$m_{Z'}/g' > 7 \text{ TeV}. \tag{6}$$

The mixing between the SM complex $SU(2)_L$ doublet and complex scalar singlet is controlled by the coupling λ_3 as shown in Eq. (3). This mixing can be expressed by the mass matrix ϕ and χ

$$\frac{1}{2}m^2(\phi,\chi) = \begin{pmatrix} \lambda_1 v^2 & \frac{\lambda_3}{2}vv' \\ \frac{\lambda_3}{2}vv' & \lambda_2 v'^2 \end{pmatrix}. \tag{7}$$

Therefore, the mass eigenstates fields H and H' are given by

$$\begin{pmatrix} H \\ H' \end{pmatrix} = \begin{pmatrix} \cos\alpha & -\sin\alpha \\ \sin\alpha & \cos\alpha \end{pmatrix} \begin{pmatrix} \phi \\ \chi \end{pmatrix}, \tag{8}$$

where the mixing angle α is defined by

$$\tan 2\alpha = \frac{|\lambda_3| v v'}{\lambda_1 v^2 - \lambda_2 v'^2}. \tag{9}$$

The masses of H and H' are given by

$$m^2_{H,H'} = \lambda_1 v^2 + \lambda_2 v'^2 \mp \sqrt{(\lambda_1 v^2 - \lambda_2 v'^2)^2 + \lambda_3^2 v^2 v'^2}. \tag{10}$$

Here, H and H' are light and heavy Higgs bosons, respectively.

From Eqs. (9) and (10), it is straightforward to have:

$$\begin{aligned}
\lambda_1 &= \frac{m_H^2}{2v^2}\cos^2\alpha + \frac{m_{H'}^2}{2v^2}\sin^2\alpha, \\
\lambda_2 &= \frac{m_H^2}{2v'^2}\sin^2\alpha + \frac{m_{H'}^2}{2v'^2}\cos^2\alpha, \\
\lambda_3 &= \frac{(m_{H'}^2 - m_H^2)}{2vv'}\sin(2\alpha).
\end{aligned} \tag{11}$$

Because of the mixing between the two Higgs bosons H and H', the usual couplings among the SM-like Higgs H boson and the SM particles are modified. Additionally, there are new couplings among the extra Higgs H' and the SM particles, which will lead to a different Higgs phenomenology from the SM. Notice that the scalar mixing angle α is a free parameter of the model, and the light(heavy) Higgs boson couples to the new matter content proportionally to sinα (cosα). The relevant Feynman rules involved in our calculations are given in Table A.1 of App. A, which can be found in Refs. [39, 46].

III. HIGGS PRODUCTIONS IN THE B-L MODEL AT ILC

In our numerical calculations, we take the SM parameters as: m_t =172.4 GeV, $\sin^2\theta_W$ =0.23126, m_Z =91.187 GeV, m_H =125 GeV, $\alpha(m_Z)$=1/128 [56]. For the $B-L$ parameters, the mixing angle α, the gauge coupling constant g', the mixing gauge coupling $\tilde{g}$, the masses $m_{Z'}$, $m_{H'}$ and m_{ν_H} are involved. The Ref.[57] has discussed the constraints on these parameters from experiment and theory, and points out that sin$\alpha \leq 0.36$, $m_{Z'} \geq 1830$ GeV, $m_{\nu_H} \sim 500$ GeV, $m_{H'} \geq 125$ GeV. In the following calculations, we vary sinα in the range of $0.05 \leq \sin\alpha \leq 0.4$, and take $m_{Z'} = 2500$ GeV, $m_{\nu_H} = 500$ GeV, $m_{H'} = 500$ GeV, $g' = 0.3$, $\tilde{g} = -0.1$. All the numerical results are done by using CalcHEP 3.6.25 package [58].

A. Single Higgs boson productions

In Fig.1 and Fig.2, we show the lowest-order Feynman diagrams of the single Higgs boson production processes $e^+e^- \to ZH$, $e^+e^- \to \nu_e\bar{\nu}_e H$ and $e^+e^- \to t\bar{t}H$ in the $B-L$ model. In comparison with the SM, we can see that these three processes receive the additional contributions from the heavy gauge boson Z' and the modified couplings of HXX at the tree-level.

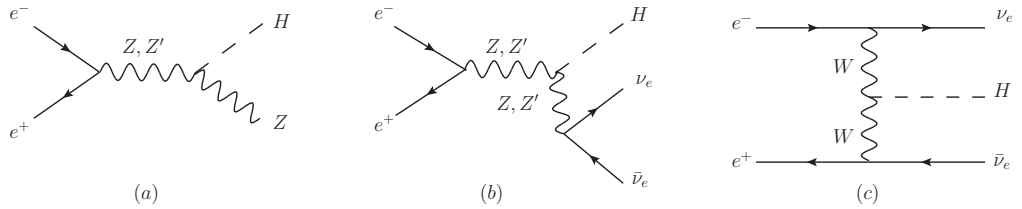

FIG. 1: Lowest-order Feynman diagrams for $e^+e^- \to ZH$(a) and $e^+e^- \to \nu_e\bar{\nu}_e H$(b,c) in the $B-L$ model.

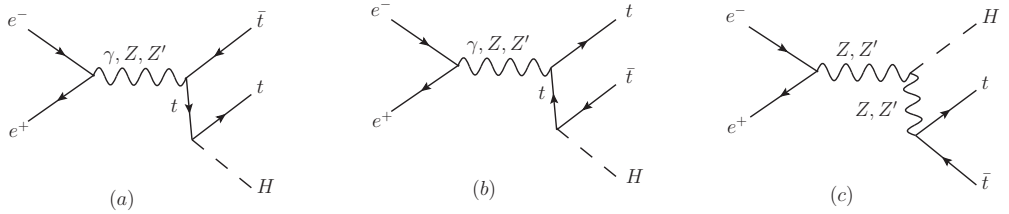

FIG. 2: Lowest-order Feynman diagrams for $e^+e^- \to t\bar{t}H$ in the $B-L$ model.

In Fig.3, we show the production cross sections σ of these three processes versus the c.m. energy $\sqrt{s}$ in the SM and $B-L$ model, respectively. We can see that the process $e^+e^- \to ZH$ reaches its maximum at ~ 250 GeV. The $\nu_e\bar{\nu}_e H$ production cross sections increase with the $\sqrt{s}$ and can take over that of the ZH process at $\sqrt{s} \geq 500$ GeV. Similar to the process $e^+e^- \to ZH$, the $t\bar{t}H$ production cross sections increase firstly and then decrease with the $\sqrt{s}$ and reaches its maximum at ~ 800 GeV. The cross sections of these three production processes in the $B-L$ model are all lower than their SM values.

Considering the polarization of the initial electron and positron beams, the cross section

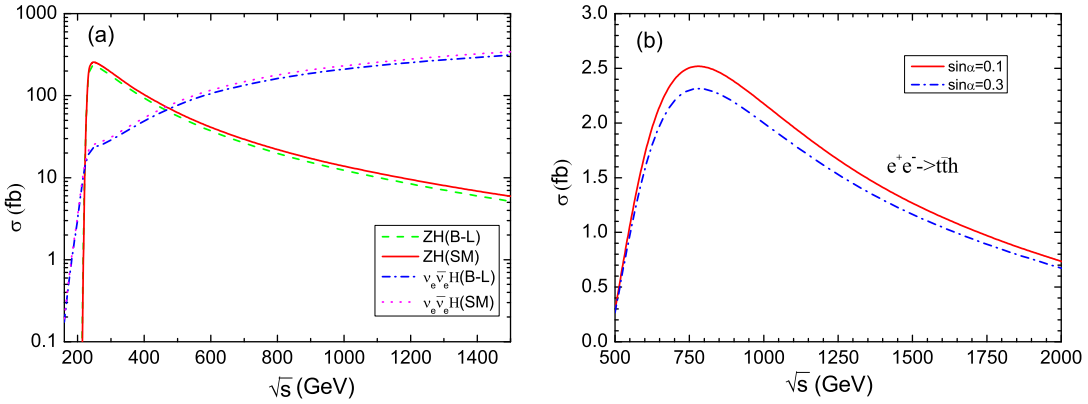

FIG. 3: The production cross section σ for the process $e^+e^- \to ZH$, $e^+e^- \to \nu_e\bar{\nu}_e H$ (a) and $e^+e^- \to t\bar{t}H$ (b) versus the c.m. energy $\sqrt{s}$ in the SM and $B-L$ model.

of a process can be expressed as [59, 60]

$$\begin{aligned}\sigma(P_{e^-}, P_{e^+}) &= \frac{1}{4}[(1+P_{e^-})(1+P_{e^+})\sigma_{RR} + (1-P_{e^-})(1-P_{e^+})\sigma_{LL} \\ &+(1+P_{e^-})(1-P_{e^+})\sigma_{RL} + (1-P_{e^-})(1+P_{e^+})\sigma_{LR}], \end{aligned} \tag{12}$$

where P_{e^-} and P_{e^+} are the polarization degree of the electron and positron beam, respectively. As in Ref. [9], we assume $P(e^-, e^+) = (-0.8, 0.3)$ at $\sqrt{s}$=250, 500 GeV and $P(e^-, e^+) = (-0.8, 0.2)$ at $\sqrt{s}$=1000 GeV in our calculations.

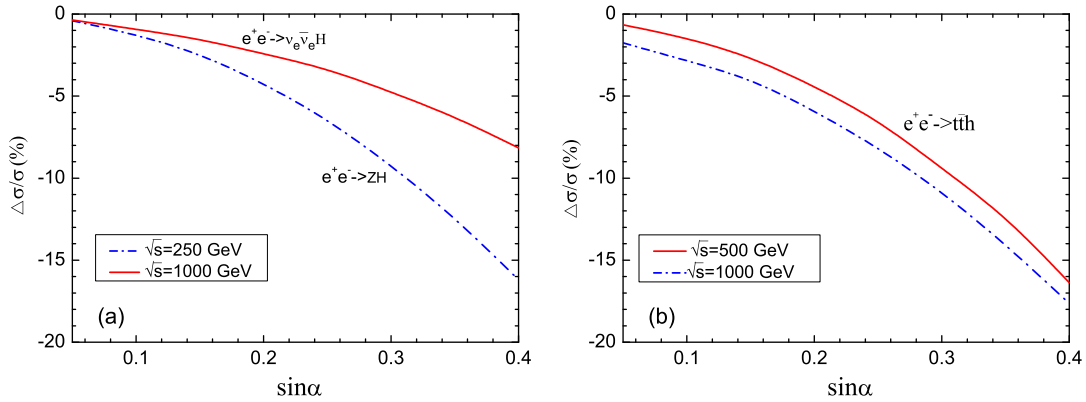

FIG. 4: The relative correction $\Delta\sigma/\sigma$ for the process $e^+e^- \to ZH$, $e^+e^- \to \nu_e\bar{\nu}_e H$ (a) and $e^+e^- \to t\bar{t}H$ (b) versus sinα for different c.m. energy $\sqrt{s}$ in the $B-L$ model.

In Fig.4, we show the relative corrections $\Delta\sigma/\sigma$=$(\sigma_{B-L} - \sigma_{SM})/\sigma_{SM}$ of the three single Higgs boson production channels versus the mixing angle sinα for $\sqrt{s} = 250, 500, 1000$

GeV at the ILC with polarized beams. For these three processes, we can see that the values of the relative corrections are all negative and increase with the sinα increasing, the $\Delta\sigma/\sigma$ of processes ZH, $\nu_e\bar{\nu}_e H$, $t\bar{t}H$ can respectively reach $-16.2\%, -8.2\%, -16.4\%$. Due to the fact that the effects of the heavy gauge boson Z' decouple, the relative corrections $\Delta\sigma/\sigma$ are insensitive to the $m_{Z'}$, so we do not show the dependence of the relative corrections on $m_{Z'}$ here.

At the ILC with $\sqrt{s} = 250$ GeV, the total SM electroweak correction for the ZH production process is about 5% [61, 62]. Meanwhile, the ILC can measure the cross section for ZH and $\nu_e\bar{\nu}_e H$ to a relative accuracy of $2.0 - 2.6\%$ and $2.2 - 11\%$ [9]. At the ILC with $\sqrt{s} = 1000$ GeV, the expected accuracies for $t\bar{t}H$ process may achieve an even more remarkable precision of 6.3%[9]. Thus, the $B - L$ model effects on these three processes might be observed at the ILC for the large sinα.

B. Double Higgs boson productions

At the ILC, the main triple Higgs boson coupling can be studied through the double Higgs-strahlung off Z boson process $e^+e^- \to ZHH$ and double Higgs fusion process $e^+e^- \to \nu_e\bar{\nu}_e HH$. The relevant Feynman diagrams are shown in Fig.5 and Fig.6.

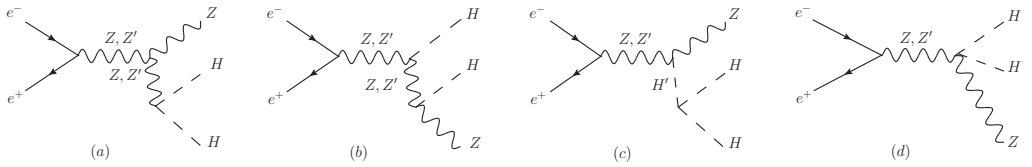

FIG. 5: Lowest-order Feynman diagrams for $e^+e^- \to ZHH$ in the $B - L$ model.

In Fig.7(a), we show the cross sections for the two processes versus the c.m. energy $\sqrt{s}$ in the SM and the $B - L$ model for sin$\alpha = 0.3$. We can see that the cross section for the process $e^+e^- \to ZHH$ reaches its maximum at around 500 GeV. It is noteworthy that the process $e^+e^- \to \nu_e\bar{\nu}_e HH$ will become sizable at $\sqrt{s} = 1000$ GeV and can be used together with the $e^+e^- \to ZHH$ process to improve the measurement of the Higgs self-coupling. Furthermore, we can see that the two processes have a similar trend in the SM and the $B - L$ model.

In Fig.7(b), we show the relative corrections of these two double Higgs production

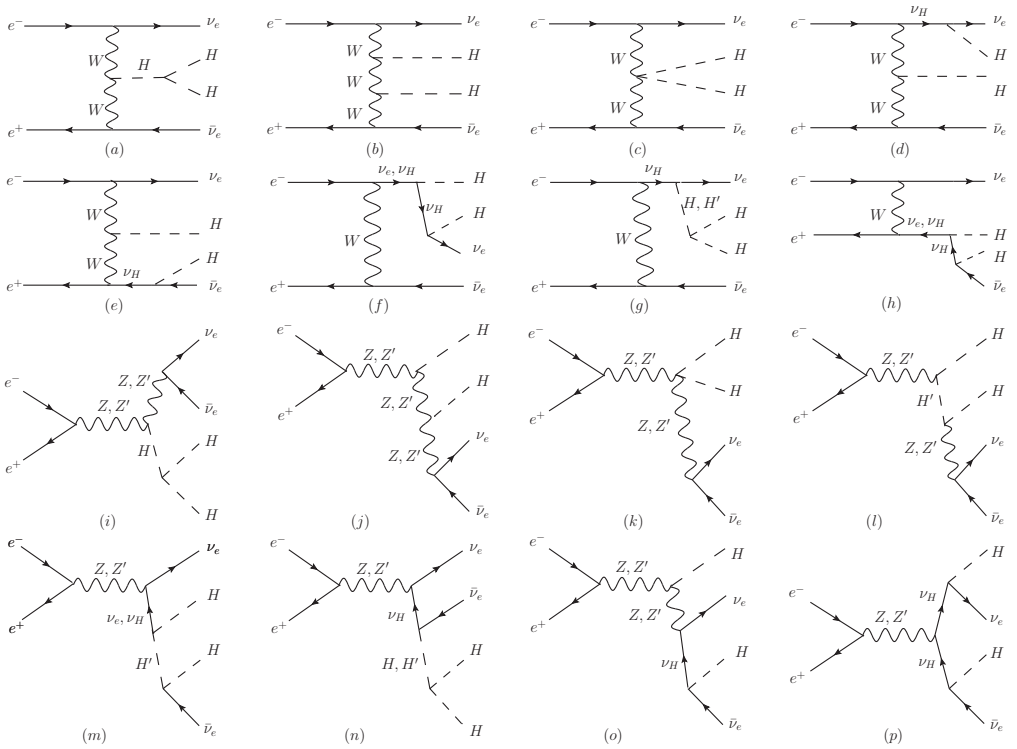

FIG. 6: Lowest-order Feynman diagrams for $e^+e^- \to \nu_e\bar{\nu}_e HH$ in the $B-L$ model.

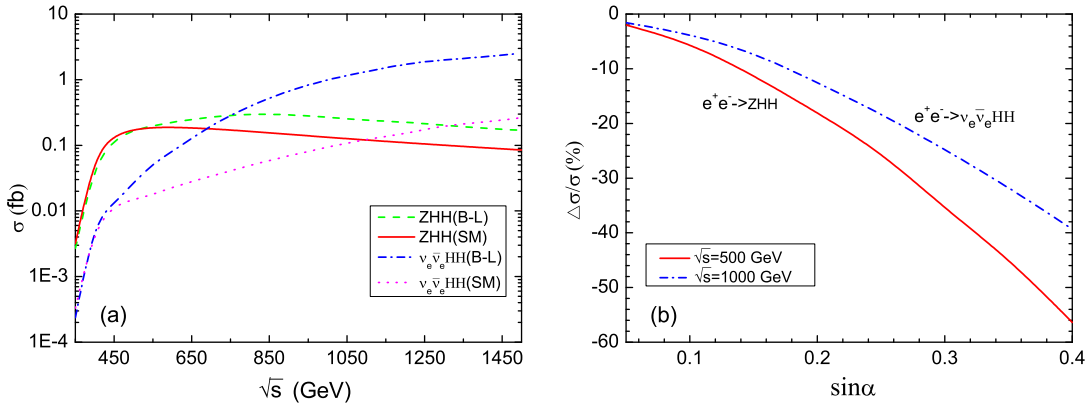

FIG. 7: The production cross section σ and the relative correction $\Delta\sigma/\sigma$ for the processes $e^+e^- \to ZHH$ and $e^+e^- \to \nu_e\bar{\nu}_e HH$ versus the c.m. energy $\sqrt{s}$ (a) and sinα (b) in the $B-L$ model.

processes versus sinα for $\sqrt{s} = 500, 1000$ GeV with polarized beams at the ILC. We can see that the relative corrections are negative and the values become larger with the increasing of the sinα, which is similar to the behavior of the single Higgs production processes mentioned above. In the region of large sinα, the $\Delta\sigma/\sigma$ of processes ZHH

and $\nu_e\bar{\nu}_e HH$ can reach -56.4% for $\sqrt{s} = 500$ GeV and -39.3% for $\sqrt{s} = 1000$ GeV, respectively. The Refs. [3, 4, 7, 63–68] suggest that the expected accuracy for the HHH coupling could be reached 50% through $pp \to HH \to bb\gamma\gamma$ at the HL-LHC with $\mathcal{L}$=3000 fb^{-1}, and this accuracy may be further improved to be around 13% at the ILC with $\sqrt{s}$=1000 GeV [3, 4, 7, 63]. By this token, the effects of the $B-L$ model might be observed through these two processes at the ILC.

IV. THE HIGGS SIGNAL STRENGTHS IN THE B-L MODEL

In order to provide more information for probing the Higgs boson processes, we give the Higgs signal strengths in the $B-L$ model. Considering the Higgs boson decay mode, the signal strengths can be defined as

$$\mu_i = \frac{\sigma_{B-L} \times BR(H \to i)_{B-L}}{\sigma_{SM} \times BR(H \to i)_{SM}}, \tag{13}$$

where i denotes a possible final state of the SM fermion and boson pairs.

TABLE I: Expected accuracies for cross section times branching ratio measurements for the 125 GeV Higgs boson [9].

	$\Delta(\sigma \cdot BR)/(\sigma \cdot BR)$								
$\mathcal{L}$ and $\sqrt{s}$ (P_{e^-}, P_{e^+})	250 fb^{-1} at 250 GeV (-0.8, +0.3)		500 fb^{-1} at 500 GeV (-0.8, +0.3)				1000 fb^{-1} at 1000 GeV (-0.8, +0.2)		
mode	ZH	$\nu_e\bar{\nu}_e H$	ZH	$\nu_e\bar{\nu}_e H$	$t\bar{t}H$	ZHH	$\nu_e\bar{\nu}_e H$	$t\bar{t}H$	$\nu_e\bar{\nu}_e HH$
$H \to b\bar{b}$	1.1%	10.5%	1.8%	0.66%	35%	64%	0.47%	8.7%	38%
$H \to c\bar{c}$	7.4%	-	12%	6.2%	-	-	7.6%	-	-
$H \to gg$	9.1%	-	14%	4.1%	-	-	3.1%	-	-
$H \to WW^*$	9.1%	-	9.2%	2.6%	-	-	3.3%	-	-
$H \to \tau^+\tau^-$	4.2%	-	5.4%	14%	-	-	3.5%	-	-
$H \to ZZ^*$	19%	-	25%	8.2%	-	-	4.4%	-	-
$H \to \gamma\gamma$	29-38%	-	29-38%	20-26%	-	-	7-10%	-	-

The expected accuracies for $\Delta(\sigma \cdot BR)/(\sigma \cdot BR)$ measurements for $m_H = 125$ GeV at the ILC are shown in Table I. Due to the $b\bar{b}$ decay mode is more easily achievable

than other modes [8, 9], we only consider this decay mode in the following section. The expected precision limits of the $b\bar{b}$ mode respectively correspond to the blue dash-dot lines in the numerical figures.

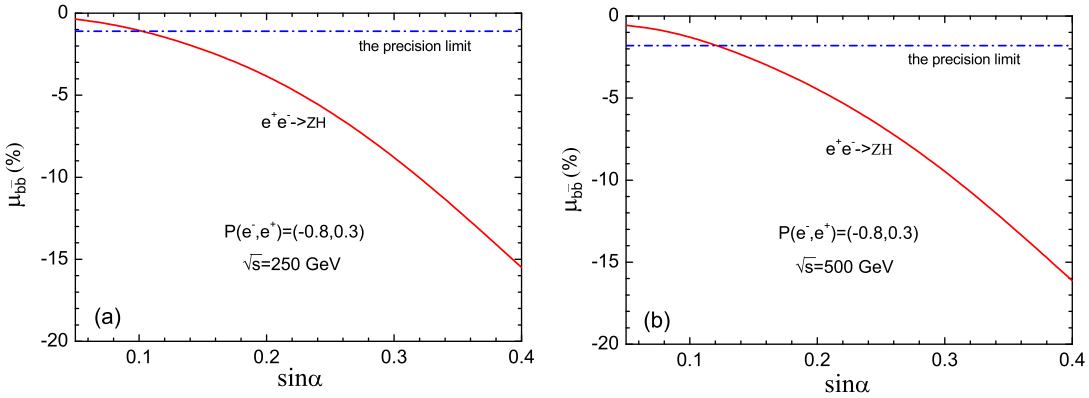

FIG. 8: Higgs signal strengths $\mu_{b\bar{b}}$ for the process $e^+e^- \to ZH$ versus sinα for $\sqrt{s} = 250$ GeV (a) and $\sqrt{s} = 500$ GeV (b) in the $B - L$ model.

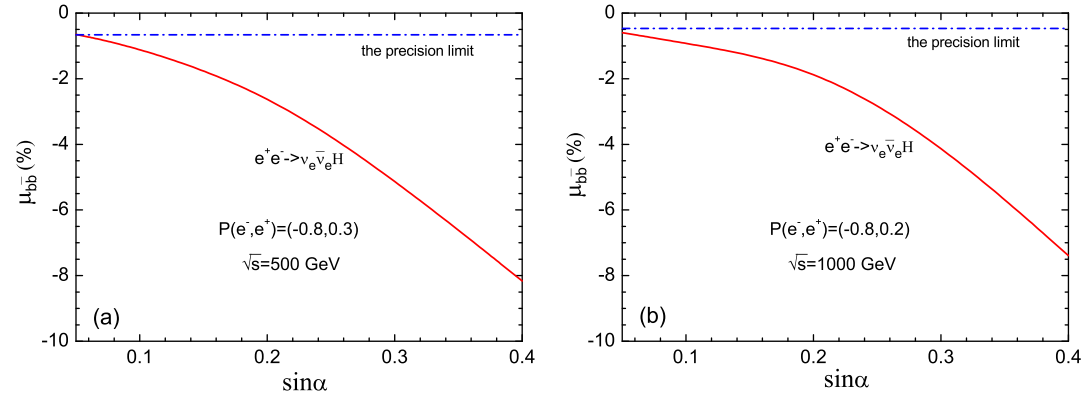

FIG. 9: Higgs signal strengths $\mu_{b\bar{b}}$ for the process $e^+e^- \to \nu_e\bar{\nu}_e H$ versus sinα for $\sqrt{s} = 500$ GeV (a) and $\sqrt{s} = 1000$ GeV (b) in the $B - L$ model.

In Fig.8, we show the dependence of the Higgs signal strengths $\mu_{b\bar{b}}$ on the parameter sinα for the process $e^+e^- \to ZH$ with polarized beams. From Table I, we can see that the 1.1(1.8)% accuracy for this mode are expected at $\sqrt{s} = 250(500)$ GeV, and the contributions of the $B - L$ model might be detected by the measurement of the $b\bar{b}$ signal rate in the future ILC experiments for sin$\alpha > 0.1$.

In Fig.9, we show the dependence of the Higgs signal strengths $\mu_{b\bar{b}}$ on the parameter

sinα for the processes $e^+e^- \to \nu_e\bar{\nu}_e H$ with polarized beams. From Table I, we can see that the 0.66(0.47)% accuracy for the processes $e^+e^- \to \nu_e\bar{\nu}_e H$ are expected at $\sqrt{s} = 500(1000)$ GeV. This accuracy is so high that almost any deviation from the SM prediction can be detected by the measurement of the $b\bar{b}$ signal rate. Conversely, the ILC measurement will give strong bound on the $B - L$ parameter if this effect can not be detected.

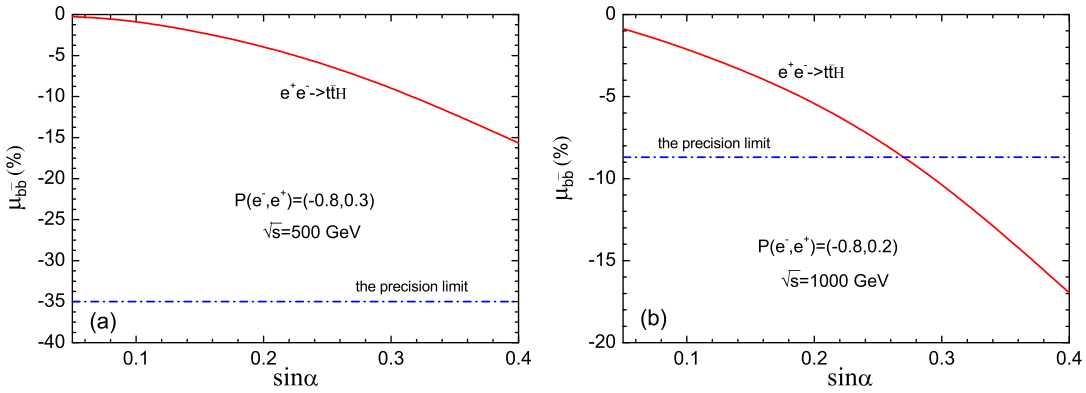

FIG. 10: Higgs signal strengths $\mu_{b\bar{b}}$ for the process $e^+e^- \to t\bar{t}H$ versus sinα for $\sqrt{s} = 500$ GeV (a) and $\sqrt{s} = 1000$ GeV (b) in the $B - L$ model.

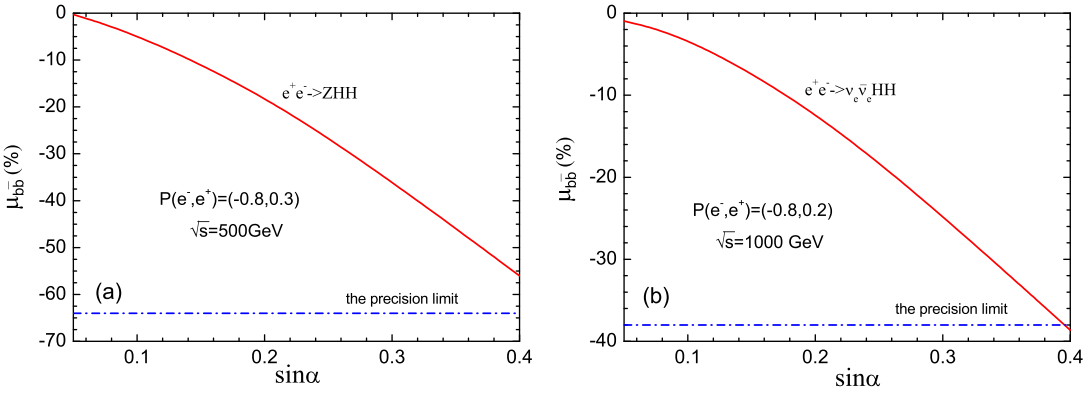

FIG. 11: Higgs signal strengths $\mu_{b\bar{b}}$ for the process $e^+e^- \to ZHH$ at $\sqrt{s} = 500$ GeV (a) and $e^+e^- \to \nu_e\bar{\nu}_e HH$ at $\sqrt{s} = 1000$ GeV (b) versus sinα in the $B - L$ model.

In Fig.10, we show the dependence of the Higgs signal strengths $\mu_{b\bar{b}}$ on the parameter sinα for the processes $e^+e^- \to t\bar{t}H$ with polarized beams. From Table I, we can see that the accuracy for top Yukawa coupling is about 35% at $\sqrt{s} = 500$ GeV, which is difficult to observe the $B - L$ effect on the process $e^+e^- \to t\bar{t}H$ via the $b\bar{b}$ channel. However, this

accuracy can be improved to 8.7% at $\sqrt{s} = 1000$ GeV so that the $B - L$ effect of this process may be detected at the high energy ILC for $\sin\alpha \geq 0.3$.

In Fig.11, we show the dependence of the Higgs signal strengths $\mu_{b\bar{b}}$ on the parameter $\sin\alpha$ for the double Higgs production processes $e^+e^- \to ZHH$ and $e^+e^- \to \nu_e\bar{\nu}_e HH$ with polarized beams, respectively. We can see that the Higgs signal strengths $\mu_{b\bar{b}}$ of these two processes are both below the expected precision limits so that these effects will be hard to be observed at the ILC.

V. SUMMARY

Under current constraints, we investigated the single and double Higgs boson production processes $e^+e^- \to ZH$, $e^+e^- \to \nu_e\bar{\nu}_e H$, $e^+e^- \to t\bar{t}H$, $e^+e^- \to ZHH$ and $e^+e^- \to \nu_e\bar{\nu}_e HH$ in the $B - L$ model at the ILC. We calculated the production cross sections and the relative corrections with the polarized beams for $\sqrt{s}$=250 GeV, 500 GeV, 1000 GeV. We also studied the signal rates with the SM-like Higgs boson decaying to $b\bar{b}$, and performed a simulation by using the projected sensitivities given by the ILC. For the three single Higgs boson production processes, we found that the processes $e^+e^- \to ZH$ and $e^+e^- \to \nu_e\bar{\nu}_e H$ might approach the observable threshold of the ILC in the allowed parameter space. For the two double Higgs boson production processes, we found that the Higgs signal strengths $\mu_{b\bar{b}}$ of them are all out of the observed threshold of the ILC in most regions of parameter space so that the effects will be difficult to be observed at the ILC.

Acknowledgement

We would like to thank Lorenzo Basso and Alexander Belyaev for providing the CalcHep Model Code and the helpful suggestions. This work is supported by the Joint Funds of the National Natural Science Foundation of China under grant No. U1404113, by the National Natural Science Foundation of China under Grant Nos. 11405047, 11305049, by the China Postdoctoral Science Foundation under Grant No. 2014M561987.

Appendix

TABLE II: The relevant Feynman rules for single and double Higgs boson processes in the minimal $B-L$ model at the ILC.

vertices	Variational derivative of Lagrangian by fields
$H \quad Z_\mu \quad Z_\nu$	$\frac{c_\alpha e m_W}{c_w^2 s_w} g^{\mu\nu}$
$H \quad Z_\mu \quad Z'_\nu$	$\frac{1}{c_w e s_w}[s_w^2 s_p s_\alpha c_p m_W \tilde{g}^2 - s_w^4 s_p c_\alpha c_p m_W \tilde{g}^2$
	$-s_w c_w c_\alpha e m_w \tilde{g} + 2 s_w s_p^2 c_w c_\alpha e m_w \tilde{g} - s_p c_\alpha c_p e^2 m_w$
	$-8 s_w s_\alpha s_p c_p e g'^2 v' + 8 s_w^3 s_\alpha s_p c_p e g'^2 v'] g^{\mu\nu}$
$H \quad Z'_\mu \quad Z'_\nu$	$-8 s_\alpha g_1'^2 x g^{\mu\nu}$
$H \quad W_\mu^+ \quad W_\nu^-$	$\frac{c_\alpha e m_W}{s_w} g^{\mu\nu}$
$H' \quad Z_\mu \quad Z_\nu$	$\frac{e m_W s_\alpha}{c_w^2 s_w} g^{\mu\nu}$
$\bar{t} \quad t \quad H$	$-\frac{1}{2}\frac{c_\alpha e m_t}{m_W s_w}$
$\bar{t} \quad t \quad Z_\mu$	$-\frac{1}{6}\frac{e}{c_w s_w}\gamma^\mu\big((3-4s_w^2)\frac{(1-\gamma^5)}{2} - 4s_w^2\frac{(1+\gamma^5)}{2}\big)$
$\bar{t} \quad t \quad Z'_\mu$	$-\frac{1}{3} g'_1 \gamma^\mu$
$\nu l_a^i \quad \nu l_b^i \quad Z_\mu$	$\frac{1}{2}\frac{c_{ai}^2 e}{c_w s_w}\gamma^\mu_{ac}\gamma^5_{cb}$
$\nu l_a^i \quad \nu l_b^i \quad Z'_\mu$	$-(1-2s_{ai}^2) g'_1 \gamma^\mu_{ac}\gamma^5_{cb}$
$\nu l_a^i \quad \nu h_b^1 \quad H$	$-\frac{1}{2}\frac{1}{v'}\big((1-2s_{ai}^2)c_\alpha\sqrt{2}v' y_i^\nu \delta_{ab} + 2 s_\alpha s_{ai} c_{ai} m_{\nu_i}\delta_{ab}\big)$
$\nu l_a^i \quad \nu h_b^1 \quad H'$	$-\frac{1}{2}\frac{1}{v'}\big((1-2s_{ai}^2)s_\alpha\sqrt{2}v' y_i^\nu \delta_{ab} - 2 s_{ai} c_\alpha c_{ai} m_{\nu_i}\delta_{ab}\big)$
$H \quad H \quad H$	$-3\frac{1}{e}\big(4c_\alpha^3 s_w m_W \lambda_1 - 2 s_\alpha^3 e\lambda_2 v' - c_\alpha^2 s_\alpha e\lambda_3 v'$
	$+2 s_w s_\alpha^2 c_\alpha m_W \lambda_3\big)$
$H \quad H \quad H'$	$-\frac{1}{e}\big(12 c_\alpha^2 s_w s_\alpha m_W\lambda_1 + 6 s_\alpha^2 c_\alpha e\lambda_2 v' + (1-3s_\alpha^2)c_\alpha e\lambda_3 v'$
	$-2(2-3s_\alpha^2)s_w s_\alpha m_W \lambda_3\big)$
$H \quad H \quad W_\mu^+ \quad W_\nu^-$	$\frac{1}{2}\frac{c_\alpha^2 e^2}{s_w^2} g^{\mu\nu}$
$H \quad H \quad Z_\mu \quad Z_\nu$	$\frac{1}{2}\frac{c_\alpha^2 e^2}{c_w^2 s_w^2} g^{\mu\nu}$

Here, e is the electric charge, $s_w(c_w) \Rightarrow \sin\theta_W(\cos\theta_W)$, $s_\alpha(c_\alpha) \Rightarrow \sin\alpha(\cos\alpha)$, $s_{\alpha i}(c_{\alpha i})$ is the sinus(cosinus) of the "see-saw" mixing of the i^{th} neutrino generation, $s_p = \frac{1}{2}\sin(\arcsin(s_n/\sqrt{s_n^2+c_n^2}))$, $c_p = \sqrt{1-s_p^2}$, $s_n = 2\tilde{g}\sqrt{(\frac{e}{s_w})^2+(\frac{e}{c_w})^2}$, $c_n = \tilde{g}^2 + 16 g'^2(\frac{v'}{v})^2 - (\frac{e}{s_w})^2 - (\frac{e}{c_w})^2$.

[1] ATLAS Collaboration (G. Aad *et al.*), *Phys. Lett. B* **716**, 1-29 (2012).

[2] CMS Collaboration (S. Chatrchyan *et al.*), *Phys. Lett. B* **716**, 30-61 (2012).

[3] T. Han, Z. Liu and J. Sayre, *Phys. Rev. D* **89**, 113006 (2014).

[4] P. Bechtle, S. Heinemeyer, O. Stal, T. Stefaniak and G. Weiglein, *JHEP* **1411**, 039 (2014).

[5] C. Englert, A. Freitas, M. Muhlleitner *et al.*, *J. Phys. G* **41**, 113001 (2014).

[6] M. E. Peskin, arXiv:1312.4974 [hep-ph].

[7] S. Dawson, A. Gritsan, H. Logan *et al.*, arXiv:1310.8361 [hep-ex].

[8] T. Behnke, J. E. Brau, B. Foster *et al.*, arXiv:1306.6327 [acc-ph].

[9] H. Baer, T. Barklow, K. Fujii *et al.*, arXiv:1306.6352 [hep-ph].

[10] D. M. Asner, T. Barklow, C. Calancha *et al.*, arXiv:1310.0763 [hep-ph].

[11] B. A. Kniehl, *Int. J. Mod. Phys. A* **17**, 1457-1476 (2002).

[12] F. Jegerlehner, O. Tarasov, *Nucl. Phys. Proc. Suppl.* **116**, 83-87 (2003).

[13] G. Belanger *et al.*, *Phys. Lett. B* **559**, 252-262 (2003).

[14] F. Boudjema *et al.*, *Phys. Lett. B* **600**, 65-76 (2004).

[15] A. Denner, S. Dittmaier, M. Roth and M. M. Weber, *Phys. Lett. B* **560**, 196-203 (2003).

[16] A. Denner, S. Dittmaier, M. Roth and M. M. Weber, *Nucl. Phys. B* **660**, 289-321 (2003).

[17] P. S. Bhupal Dev *et al.*, *Phys. Rev. Lett.* **100**, 051801 (2008).

[18] H. Eberl, W. Majerotto and V. C. Spanos, *Nucl. Phys. B* **657**, 378-396 (2003).

[19] T. Hahn, S. Heinemeyer and G. Weiglein, *Nucl. Phys. B* **652**, 229-258 (2003).

[20] J. J. Cao, C. C. Han, J. Ren *et al.*, arXiv:1410.1018 [hep-ph].

[21] A. GutiLérrez-RodrLíguez and M. A. Hernández-Ruiz, *Adv. High Energy Phys.* **2015**, 593898 (2015).

[22] S. Banerjee *et al.*, *Phys. Rev. D* **92**, 075002 (2015).

[23] C. -X. Yue, S. Z. Wang and D. Q. Yu, *Phys. Rev. D* **68**, 115004 (2003).

[24] C. -X. Yue, W. Wang, Z. J. Zong and F. Zhang, *Eur. Phys. Jour. C* **42**, 331 (2005).

[25] X. L. Wang, Y. -B. Liu, J. H. Chen and H. Yang, *Eur. Phys. Jour. C* **49**, 593-597 (2007).

[26] S. L. Hu, N. Liu, J. Ren and L. Wu, *J. Phys. G* **41**, 125004 (2014).

[27] N. Liu, J. Ren, L. Wu , P. W. Wu and J. M. Yang, *JHEP* **1404**, 189 (2014).

[28] B. F. Yang, J. Z. Han, S. H. Zhou and N. Liu, *J. Phys. G* **41**, 075009 (2014).

[29] S. Antusch, E. Cazzato and O. Fischer, *JHEP* **1604**, 189 (2016).

[30] L. Wang, W. Y. Wang, J. M, Yang and H. J. Zhang, *Phys. Rev. D* **75**, 074006 (2007).

[31] J. F. Shen, J. Cao and L. B. Yan, *Europhys. Lett.* **91**, 51001 (2010).

[32] N. Liu, S. L. Hu, B. F. Yang and J. Z. Han, *JHEP* **1501**, 008 (2015).

[33] B. F. Yang, Z. Y. Liu, N. Liu and J. Z. Han, *Eur. Phys. Jour. C* **74**, 3203 (2014).

[34] B. F. Yang, J. Z. Han and N. Liu, *JHEP* **1504**, 148 (2015).

[35] L. Wu, *JHEP* **1502**, 061 (2015).

[36] Y.-B. Liu and Z.-J. Xiao, *J. Phys. G* **42**, 065005 (2015).

[37] J. Z. Han, S. F. Li, B. F. Yan and N. Liu, *Nucl. Phys. B* **896**, 200-211 (2015).

[38] S. Khalil, *J. Phys. G* **35**, 055001 (2008).

[39] L. Basso, arXiv:1106.4462.

[40] W. Emam and S. Khalil, *Eur. Phys. Jour. C* **52**, 625-633 (2007).

[41] L. Basso, A. Belyaev, S. Moretti and C. H. Shepherd-Themistocleous, *Phys. Rev. D* **80**, 055030 (2009).

[42] L. Basso, A. Belyaev, S. Moretti and G. M. Pruna, *JHEP* **0910**, 006 (2009).

[43] P. Fileviez Perez, T. Han, and T. Li, *Phys. Rev. D* **80**, 073015 (2009).

[44] L. Basso, S. Moretti, and G. M. Pruna, *Eur. Phys. Jour. C* **71**, 1724 (2011).

[45] L. Basso, S. Moretti and G. M. Pruna, *Phys. Rev. D* **83**, 055014 (2011).

[46] G. M. Pruna, arXiv:1106.4691 [hep-ph].

[47] C. Englert, T. Plehn, D. Zerwas and P. M. Zerwas, *Phys. Lett. B* **703**, 298-305 (2011).

[48] V. V. Khoze and G. Ro, *JHEP* **1310**, 075 (2013).

[49] J. Hernández López and J. Orduz-Ducuara, *J. Phys. Conf. Ser.* **468**, 012012 (2013).

[50] R. Marshak and R. N. Mohapatra, *Phys. Lett. B* **91**, 222-224 (1980).

[51] R. N. Mohapatra and R. Marshak, *Phys. Rev. Lett.* **44**, 1316-1319 (1980).

[52] C. Wetterich, *Nucl. Phys. B* **187**, 343-375 (1981).

[53] A. Masiero, J. Nieves and T. Yanagida, *Phys. Lett. B* **116**, 11-15 (1982).

[54] R. N. Mohapatra and G. Senjanovic, *Phys. Rev. D* **27**, 254 (1983).

[55] G. Cacciapaglia, C. Csaki, G. Marandella and A. Strumia, *Phys. Rev. D* **74**, 033011 (2006).

[56] Particle Data Group collaboration (K. A. Olive *et al.*), *Chin. Phys. C* **38**, 090001 (2014).

[57] S. Banerjee, M. Mitra and M. Spannowsky, *Phys. Rev. D* **92**, 055013 (2015).

[58] A. Belyaev, N. D. Christensen and A. Pukhov, *Comput. Phys. Commun.* **184**, 1729 (2013).

[59] G. Moortgat-Pick, T. Abe, G. Alexander *et al.*, *Phys. Rept.* **460**, 131 (2008).

[60] J. J. Cao, Z. X. Heng, L. Wu and J. M. Yang, *Phys. Rev. D* **81**, 014016 (2010).

[61] A. Denner, J. Kublbeck, R. Mertig and M. Bohm, *Z. Phys. C* **56**, 261 (1992).

[62] C. Englert and M. McCullough, *JHEP* **1307**, 168 (2013).

[63] M. E. Peskin, arXiv:1312.4974 [hep-ph].

[64] F. Goertz, A. Papaefstathiou, L. L. Yang and J. Zurita, *JHEP* **1306**, 016 (2013).

[65] R. S. Gupta, H. Rzehak and J. D. Wells, *Phys. Rev. D* **88**, 055024 (2013).

[66] A. J. Barr, M. J. Dolan, C. Englert and M. Spannowsky, *Phys. Lett. B* **728**, 308-313 (2014).

[67] V. Barger, L. L. Everett, C. B. Jackson and G. Shaughnessy, *Phys. Lett. B* **728**, 433 (2014).

[68] D. E. F. de Lima, A. Papaefstathiou and M. Spannowsky, *JHEP* **1408**, 030 (2014).